

# Preparation and characterization of zinc oxide doped with ferrite and chromium

Cite as: AIP Conference Proceedings **1862**, 030062 (2017); <https://doi.org/10.1063/1.4991166>  
Published Online: 10 July 2017

M. Ginting, S. Taslima, K. Sebayang, et al.



View Online



Export Citation

## ARTICLES YOU MAY BE INTERESTED IN

[Impact of crystalline defects and size on X-ray line broadening: A phenomenological approach for tetragonal SnO<sub>2</sub> nanocrystals](#)

AIP Advances **5**, 057137 (2015); <https://doi.org/10.1063/1.4921452>

[A comprehensive review of ZnO materials and devices](#)

Journal of Applied Physics **98**, 041301 (2005); <https://doi.org/10.1063/1.1992666>

[Growth of residual stress-free ZnO films on SiO<sub>2</sub>/Si substrate at room temperature for MEMS devices](#)

AIP Advances **5**, 067140 (2015); <https://doi.org/10.1063/1.4922911>

Lock-in Amplifiers  
up to 600 MHz



Zurich  
Instruments



# Preparation and Characterization of Zinc Oxide Doped with Ferrite and Chromium

M. Ginting<sup>1, a)</sup>, S. Taslima<sup>2</sup>, K. Sebayang<sup>2</sup>, D. Aryanto<sup>1</sup>, T. Sudiro<sup>1</sup>,  
and P. Sebayang<sup>1</sup>

<sup>1</sup>Research Center for Physics, LIPI, Serpong 15314, Indonesia

<sup>2</sup>Faculty of Graduate Study, University of Sumatera Utara, Medan 20155, Indonesia

<sup>a)</sup>Corresponding author: masno.ginting@gmail.com

**Abstract.** In this paper, the effect of doping concentrations of Fe and Cr on ZnO powder was studied by using X-ray diffraction (XRD). The ZnO was doped using solid state reaction method with High Speedshaker Mill (HSM) and continued with sintering at 900°C for 4 hours. Samples doped with Fe and Cr have polycrystalline hexagonal wurtzite structure. XRD pattern of ZnO doped with Fe is not far different from that with Cr. The intensity decrease and the peak shifted to a higher  $2\theta$  angle indicate the change in the crystal parameters such as lattice parameters, crystalline sizes, and d-spacing.

## INTRODUCTION

ZnO is an n-type semiconductor with a direct band gap of 3.37 eV at room temperature and has a large exciton binding energy (60 meV). It has the potential for a wide range of optoelectronic applications, solar cells, LEDs, UV lasers and gas sensors [1-2]. In recent years, ZnO was intensively studied as a material dilute magnetic semiconductor [3]. When ZnO is doped with the transition metal ions such as Mn, Fe, Cu, Cr, Co, and V, it shows ferromagnetic properties [4]. This occurs due to the spin exchange interaction, so that the ZnO shows its magnetic properties [5]. Chromium (Cr) and iron (Fe) are a transition metal with a unique chemical stability [6]. Room-temperature ferromagnetism (RTFM) in ZnO: Fe and ZnO: Cr has been widely studied, but only a few studies had been done on the structure of the ZnO after doping. It is well known that the nature of the material structures will affect other physical properties. Previous studies [6-10] suggest that the addition of doping Fe, Cr, or both, affect the structure of the resulted crystals. The structural changes of the material will change its magnetic and electrical properties.

Several methods have been used for the fabrication of ZnO doping transition metals with Fe and Cr, such as: sol-gel [6, 11], coprecipitation [12], solid state reaction [7-8], sputtering [1] and hydrothermal [13]. However, the method of solid state reaction is less expensive, simple in preparation and could be more easily to scaled-up [14]. This paper reports the XRD study on the fabricated ZnO: Fe and ZnO: Cr using solid state reaction.

## EXPERIMENTAL DETAIL

The main material for this study was source-based ceramic oxide (ZnO), while doping material (Fe and Cr) was used a pure metal. Doping concentrations were varied from 2.5 to 4.5 at.% and samples information are shown in Table 1. The sample was prepared by wet milling using toluene as a solvent by inserting ZnO powder, dopant, and stainless steel ball into a cylindrical stainless steels vial and then milled with HSM for three hours. The ratio of powder and ball used is 1:10. The sample was then heated in an oven at 100°C for 3 hours. The powder was sintered at 900°C for 4 hours in atmosphere condition. The structure of ZnO doped with Fe and Cr were identified by using XRD (Smartlab-Rigaku with  $\text{CuK}\alpha$  radiation,  $\lambda = 1.5406 \text{ \AA}$ ). Crystal size, lattice parameters (a and c), d-spacing, volume and Zn-O bond distance are calculated from the results of XRD analysis.

## RESULTS AND DISCUSSION

Figure 1 shows the XRD patterns of pure ZnO and ZnO doped with Fe (Fig. 1a), detail of the XRD pattern observation at the angle of  $20^\circ$  to  $65^\circ$  (Fig. 1b) and detail observation of the ZnO (002) peak (Fig. 1c). Pure ZnO and doped ZnO appeared as three dominant peaks at an angle  $2\theta$  of  $31.81^\circ$ ,  $34.47^\circ$  and  $36.29^\circ$ , consecutively identified as the plane of (100), (002) and (101) (JCPDS No. 00-005-0664). There are also peaks at (102), (110), (103), (200), (112) and (201) with a low intensity. These results confirm that the preparation of pure ZnO and doped ZnO with Fe has a wurtzite hexagonal structure [15]. More detailed observations of XRD pattern in Fig. 1b, shows the peaks at around  $2\theta$  angle of  $30.32^\circ$ ,  $35.1^\circ$ , and  $62^\circ$  indicating  $\text{ZnFe}_2\text{O}_4$  phases (JCPDS No. 01-086-0508). The appearance of  $\text{ZnFe}_2\text{O}_4$  phases might be due to the mechanical diffusion occurred during mixing and milling process. The sintering effect is also believed to cause the Fe ion diffusion into the lattice of ZnO, as also reported in Ref. [9]. The peak intensity of  $\text{ZnFe}_2\text{O}_4$  increases with the doping concentration. The increase concentration of Fe dopant will also increase the value of Fe ions diffusion in the ZnO lattice [9]. Fig. 1c is the fitting analysis done to the plane of (002).

It can be clearly seen that there is a peak shift towards the larger  $2\theta$  angle when ZnO doped with Fe. The position change of the diffraction peaks of ZnO doped with Fe due to the additional of dopant was also observed. These results indicate that the change in the lattice parameters of ZnO is due to the diffusion of Fe ions into ZnO lattice. The

TABLE 1. Samples designation based on the doping concentration.

Sample	Material	Sample	Material
ZnO	Pure ZnO	Cr-25	ZnO-2.5 at.% Cr
Fe-25	ZnO-2.5 at.% Fe	Cr-35	ZnO-3.5 at.% Cr
Fe-35	ZnO-3.5 at.% Fe	Cr-45	ZnO-4.5 at.% Cr
Fe-45	ZnO-4.5 at.% Fe		

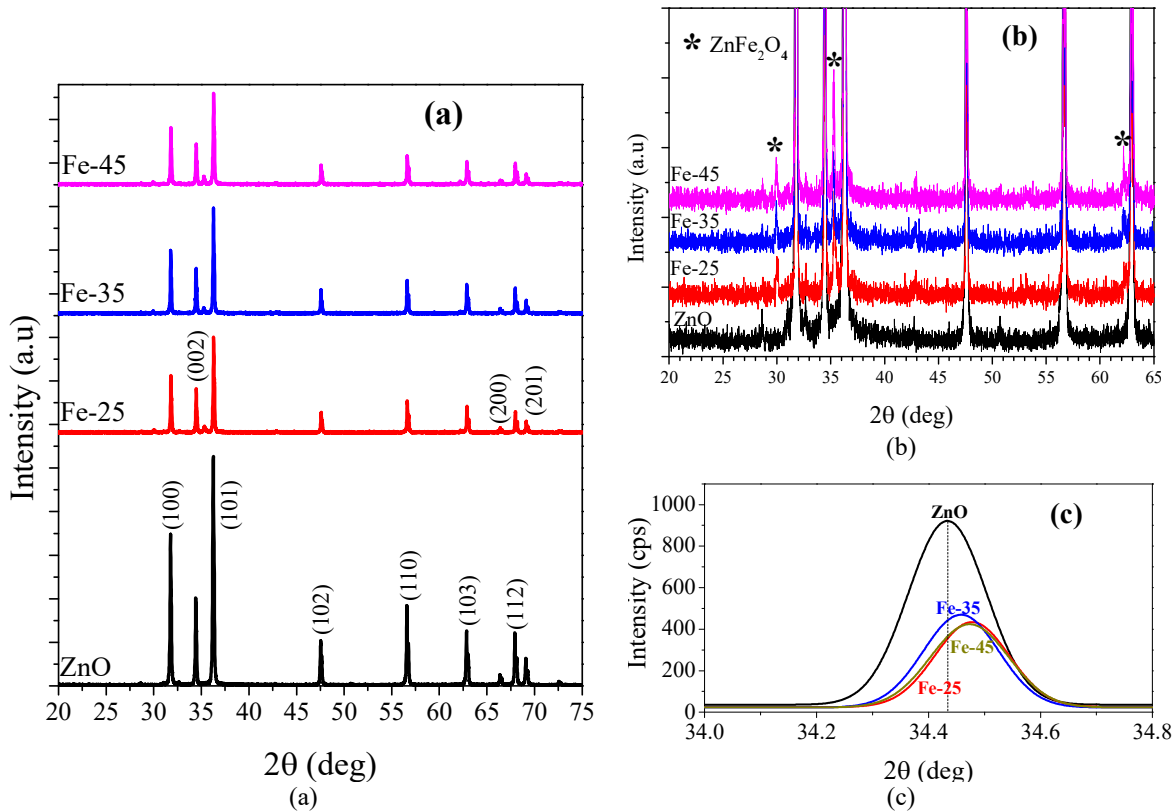


FIGURE 1. (a) XRD patterns of pure ZnO and ZnO doped with Fe, (b) detail of the XRD pattern observation angle of  $20^\circ$  to  $65^\circ$  and (c) detail observation of the ZnO (002) peak.

calculated crystal parameters such as d-spacing, the average size of the crystals, the lattice parameter, Zn-O bond length and the unit cell volume of ZnO (002) for doping ZnO Fe and Cr are shown in Table 2. The *d*-spacing of the crystal planes (002) for the hexagonal structure is determined using the Equation 1 [16].

$$\frac{1}{d^2} = \frac{a(h^2 + hk + l^2)}{(3a^2)} + \left(\frac{l^2}{c^2}\right) \quad (1)$$

where *a* and *c* are a hexagonal crystal lattice parameters, *h k l* are miller indices. The value of the *d*-spacing is closely related to the presence of strain fields within the non-equilibrium grain boundaries inside of crystallite [15].

Based on the FWHM data from the diffraction peak of (002) plane, the average crystals size (*D*) can be calculated using Debby Scherrer formula as given in Equation 2 [2],

$$D = \frac{0.9\lambda}{\beta \cos \theta} \quad (2)$$

where  $\beta$  is the FWHM of the diffraction peak (002). In this work, the crystal size of ZnO doping Fe decreased from 53.51 nm to 50.84 nm with increasing the value of Fe concentration. The same result is shown in the preparation of Fe doping ZnO with a sol-gel method reported somewhere [17]. However, a different result is obtained when the ZnO doped with Cr, in which the crystal size is directly proportional to the increase of dopant. In Ref [10], it was reported that the ZnO crystal size was reduced as the number of Cr dopant increased. This is because of the ionic radius of Cr<sup>3+</sup> smaller than that of Zn<sup>2+</sup> ions. The difference in the results might be due to the effects of heat treatment that was performed to the sample. The grain size will also be different due to the agglomeration [15].

Figure 2 shows the XRD patterns of pure ZnO and ZnO doping Cr, the detail of the XRD pattern observation angle of 20 to 65° and the detail observation of the peak of ZnO (002). From Fig. 2a, it can be seen that the XRD patterns of ZnO doped with Cr has similarities with the XRD pattern of ZnO doped with Fe. This result also confirms that ZnO doped with Cr has a wurtzite hexagonal structure [15] with the dominant peaks intensity at planes (100), (002) and (101) (JCPDS No. 00-005-0664). The appearance of ZnCr<sub>2</sub>O<sub>4</sub> secondary phase at ZnO doped with Cr is also found at angle 2θ of about 30.32°, 35.1° and 57.5° (JCPDS No. 01-087-0028). The increasing value of ion Cr dopant will affect the number of Cr ion that was entered the ZnO lattice. This can be recognized by the increase of peak intensity (Fig. 2b). While details observation peak of ZnO at (002) plane, showed that there is also a shift to the greater value of 2θ (Fig. 2c). This can be indicated as the Cr ion is successfully substituted ion Zn in ZnO lattice. The ionic radii value of Cr<sup>3+</sup> (0.64 Å) that is smaller than Zn<sup>2+</sup> ion (0.74 Å) is believed to be the cause that the peaks is shifted to a higher value of 2θ [1] also reported a similar results, with the increasing value of Cr dopant causes a shift in the diffraction peaks. Changes to the diffraction peaks may also indicate the change in crystal parameters [18].

Table 2 listed the calculated lattice parameters, such as bond length, the unit cell volume, and the average size of the crystals in the plane (002) for all samples included pure ZnO. The value of the lattice parameters for ZnO doped with Fe or Cr are smaller than the theory (JCPDS No. 00-005-0664) where the value of *a* = 3.249Å, and *c* = 5.205 Å. This confirmed that most of ion Fe or Cr was successfully substituted into the ZnO lattice. While the Zn-O bond length (*L*) can be estimated using Equation 3:

$$L = \sqrt{\left(\frac{a^2}{3}\right) + \left(\left(\frac{1}{2}\right) - u\right)^2 c^2} \quad (3)$$

where  $u = \left(\frac{a^2}{3c^2}\right) + 0.25$  is a hexagonal structure potential parameter. The volume of the unit cell (*V*) for hexagonal system is calculated from Equation 4 [16]:

$$L = 0.866 \times a^2 \times c \quad (4)$$

It is apparent in Table 2, the lattice parameters, unit cell volume, and the Zn-O bond distance changes with increasing Fe or Cr dopant. The crystal parameter value of ZnO doped with Fe or Cr, in general, is smaller than the value of pure ZnO. This indicates that the Fe<sup>3+</sup> or Cr<sup>3+</sup>, which both have an ionic radii smaller than Zn<sup>2+</sup> ions have been substituted into the ZnO lattice. Fe<sup>3+</sup> or Cr<sup>3+</sup> ions that fill the Zn<sup>2+</sup> ion lattice resulted in crystal defects and

**TABLE 2.** Calculated lattice parameters, such as bond length, the unit cell volume and the average size of the crystals in the (002) plane for samples ZnO through ZnO doped Cr-45.

Sample	FWHM (deg)	<i>d</i> -spacing (Å)	<i>D</i> (nm)	<i>a</i> (Å)	<i>c</i> (Å)	<i>L</i> (Å)	<i>V</i> (Å <sup>3</sup> )
ZnO	0.164	2.6025	50.64	3.2489	5.2049	1.9772	47.5780
Fe-25	0.155	2.5992	53.51	3.2449	5.1984	1.9747	47.4034
Fe-35	0.158	2.6007	52.66	3.2467	5.2014	1.9759	47.4819
Fe-45	0.164	2.5996	50.84	3.2454	5.1991	1.9750	47.4214
Cr-25	0.161	2.5994	51.76	3.2450	5.1985	1.9748	47.4058
Cr-35	0.160	2.6000	51.96	3.2462	5.2000	1.9755	47.4556
Cr-45	0.161	2.5993	51.80	3.2451	5.1987	1.9749	47.4100

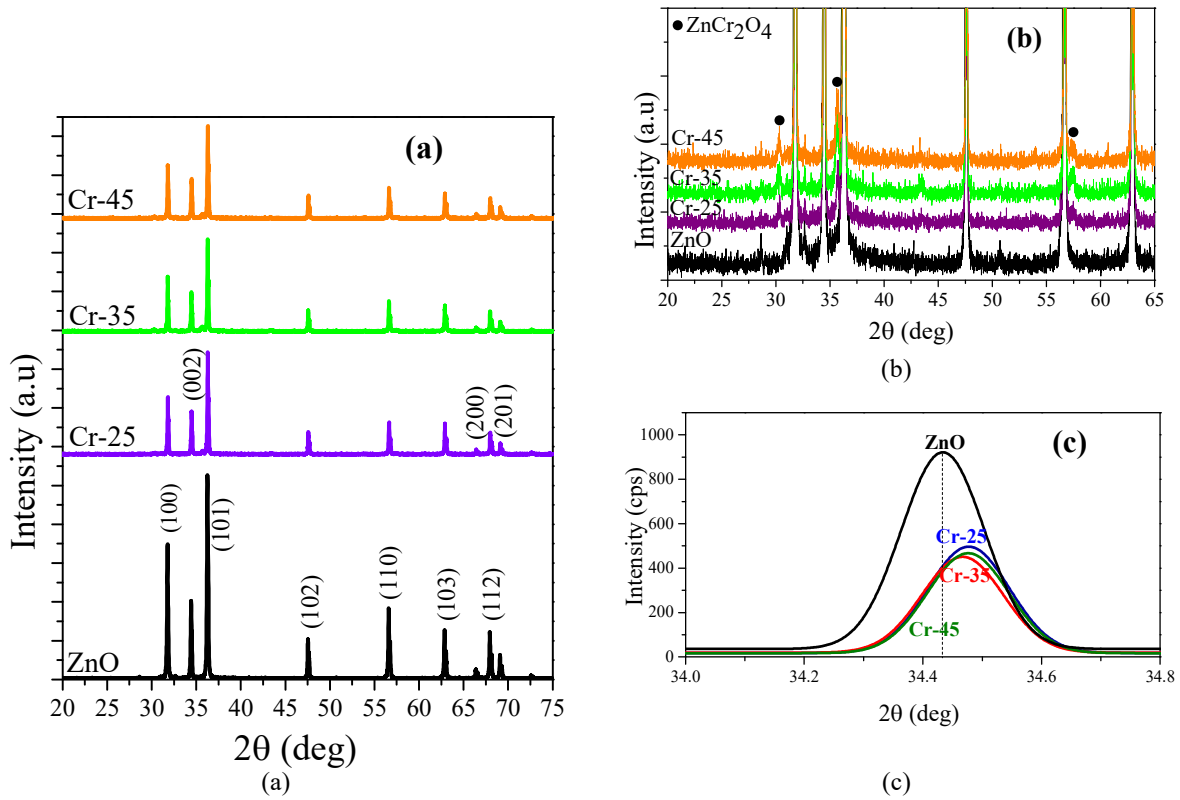


**FIGURE 2.** (a) XRD patterns of pure ZnO and ZnO doped with Cr, (b) detail of the XRD pattern observation angle of 20° to 65° and (c) detail observation of ZnO (002) peak.

charge imbalance in ZnO structure [17]. These results are shown in the XRD patterns, where the peak intensity decreases and the FWHM become wider by increasing the number of dopants.

## CONCLUSIONS

The solid state reaction preparation method and XRD characterization of ZnO doped with Fe and Cr have been successfully carried out. XRD patterns of ZnO doped with Fe or Cr showed ZnO with wurtzite hexagonal structure as the main phase. The ZnO doped with Fe produces a secondary phase ZnFe<sub>2</sub>O<sub>4</sub> while doping with Cr produce ZnCr<sub>2</sub>O<sub>4</sub> phase. Both dopants yield the ZnO with crystal sizes in the range of 46.82 to 49.42 nm. The increasing number of dopants (Fe or Cr) in ZnO crystals, resulted in the parameters changes such as *d*-spacing, lattice parameters, bond length, the unit cell volume and the size of the crystals.

## REFERENCES

1. F. Chang-feng, C. Xi-ming, L. Lan, H. Lian-fu, and W. Xiaoguo, *Optoelectron. Lett.* **6**, 1-4 (2010).
2. S. M. Salaken, E. Farzana, and J. Podder, *J. Semicond.* **34**, 073003 (2013).
3. A. Zunger, S. Lany, and H. Raebiger, *Physics* **3**, 53 (2010).
4. K. Sato and H. Katayama-Yoshida, *J. Appl. Phys.* **40**, L334-L336 (2001).
5. S. Choudhury, S. Sain, M. K. Mandal, S. K. Pradhan, and A. K. Meikap, *Mater. Res. Bull.* **77**, 138-146 (2016).
6. P. Chand, A. Gaur, and A. Kumar, *International Journal of Chemical, Molecular, Nuclear, Materials and Metallurgical Engineering* **8**, 1317-1320 (2014).
7. R. Elilarassi and G. Chandrasekaran, *Optoelectron. Lett.* **8**, 109(1-4) (2012).
8. M. Meyer and L. C. Damonte, *Powder Technol.* **286**, 371-377 (2015).
9. S. Karamat, R. S. Rawat, P. Lee, T. L. Tan, and R. V. Ramanujan, *Prog. Nat. Sci. Mater. Int.* **24**, 142-149 (2014).
10. S. A. Ansari, W. Khan, M. Chaman, and A. H. Naqvi, *Asian J. Chem.* **23**, 5622-5624 (2011).
11. W. Zhang, J. Zhao, Z. Liu, and Z. Liu, *Appl. Surf. Sci.* **284**, 49-52 (2013).
12. P. K. Sharma, R. K. Dutta, A. C. Pandey, S. Layek, and H. C. Verma, *J. Magn. Magn. Mater.* **321**, 2587-2591 (2009).
13. P. Chand, A. Gaur, and A. Kumar, *Procedia Materials Science* **10**, 97-102 (2015).
14. F. J. Owens, *J. Magn. Magn. Mater.* **321**, 3734-3737 (2009).
15. D. Aryanto *et al.*, *Proceedings of the 1<sup>st</sup> International Symposium on Current Progress in Mathematics and Sciences 2015 (ISCPMS 2015)*, Depok, 2015, edited by T. Mart and D. Triyono (AIP Publishing, New York, 2016), Vol. 1729, p. 020039.
16. V. Pazhanivelu, A. Paul Blessington Selvadurai, R. Kannan, and R. Murugaraj, *J Mater. Sci. Mater Electron.* **6**, 5549-5556 (2016).
17. M. M. Hassan, W. Khan, A. Azam, and A. H. Naqvi, *J. Lumin.* **145**, 160-166 (2014).
18. R. Bhargava, P. K. Sharma, S. Kumar, A. C. Pandey, and N. Kumar, *J. Solid State Chem.* **183**, 1400-1408 (2010).